

**PHYSICO-CHEMICAL CHARACTERISATION OF MANGROVE  
TANNINS AS CORROSION INHIBITORS**

**AFIDAH ABDUL RAHIM**

**UNIVERSITI SAINS MALAYSIA  
2005**

**PHYSICO-CHEMICAL CHARACTERISATION OF MANGROVE  
TANNINS AS CORROSION INHIBITORS**

by

**AFIDAH ABDUL RAHIM**

Thesis submitted in fulfilment of the requirements  
for the degree of Doctor of Philosophy

December 2005

## ACKNOWLEDGEMENTS

I would like to express my sincere appreciation and gratitude to my supervisors Prof. Jean Steinmetz, Assoc. Prof. Mohd Jain Noordin Md. Kassim, Assoc. Prof. Md. Sani Ibrahim and Dr. Emmanuel Rocca for the guidance, inspiration, support and patience throughout this study. I would like to acknowledge Dr. Rohana Adnan for her assistance in the molecular modelling studies.

I would like to thank the technical staff of the School of Chemical Sciences, Universiti Sains Malaysia and the Laboratoire de Chimie du Solide Mineral, Universite Henri Poincare, in particular Mr. Sobri Aziz Hassan, Mr. Ali Zaini, Mr. Aw Yeong Cheok Hoe, Mr. Alan and Mr. Jean-Paul for their help throughout the course of this study.

I would like to acknowledge the Universiti Sains Malaysia and the French Embassy for granting me the scholarship which covers my tuition fees and supports my living expenses during the term of this study.

My sincere thanks to all my friends and colleagues who never fail to help and encouraged me during my study.

Last but not least, my sincere appreciations to my husband, Abdul Rahman who constantly supports me, my children Mua'dz, Aufa and Najwa from whom I had been away and my parents for always being there for me.

## TABLE OF CONTENTS

	Page
Acknowledgements	ii
Table of contents	iii
List of Tables	viii
List of Figures	x
List of Abbreviations	xviii
Abstract	xx
Abstract (Bahasa Malaysia)	xxii
Abstract (French)	xxiv
<b>CHAPTER ONE - INTRODUCTION</b>	<b>1</b>
1.1 Mangrove forests in Malaysia	1
1.1.1 <i>Rhizophora</i> in general (Family-Rhizophoraceae)	3
1.1.2 <i>Rhizophora apiculata</i> (bakau minyak)	4
1.2 What are tannins?	6
1.2.1 Condensed tannins (or proanthocyanidins)	9
1.2.1.1 Analysis of condensed tannins	11
1.2.2 Uses of tannins	12
1.3 Corrosion inhibitors	15
1.3.1 Classification of corrosion inhibitors	15
1.3.2 Effects of inhibitors on corrosion processes	16
1.3.3 Mechanism of adsorption of inhibitors	19
1.4 Methods of evaluations of corrosion inhibition	23
1.4.1 Stern-Geary theory	24
1.4.2 Use of Tafel slopes	28

1.4.3	Polarisation resistance	29
1.5	Tannins – an alternative choice in corrosion protection	33
1.5.1	Tannins as corrosion inhibitors and rust converters	34
1.6	Objectives	41
<b>CHAPTER TWO – EXPERIMENTAL</b>		<b>42</b>
2.1	Tannin extraction and condensed tannins isolation	42
2.1.1	Prussian blue assay for total phenols	44
2.1.2	Vanillin assay for the determination of condensed tannins	44
2.1.3	Identification of condensed tannins	45
2.1.3.1	Phloroglucinol degradation	45
2.1.3.2	HPLC analysis	46
2.2	Anti-oxidant activities	48
2.2.1	Reducing power	48
2.2.2	DPPH free radical scavenging activity	48
2.2.3	ABTS free radical scavenging activity	49
2.3	Electrochemical tests	50
2.3.1	Inhibition studies of mangrove tannins	51
2.3.2	Comparison of the inhibitory action with several tannins	52
2.3.3	Synthesis of iron-tannates	53
2.3.4	Inhibitory performance of catechin, epicatechin, epigallocatechin and epicatechin gallate	53
2.3.4.1	Molecular modelling	54
2.3.5	Determination of redox potentials of flavanoid monomers and tannins	54
2.4.1	Preparation of pre-rusted steel plates	56
2.4.1.1	Inhibitory performance of mangrove tannins, mimosa tannins and phosphoric acid on pre-rusted steel	56

2.5	Phase transformation studies	57
2.5.1	Phase transformation of rust induced by tannins	57
2.5.2	Phase transformation of rust in the presence of tannins and phosphoric acid	57
2.5.3	Phase transformation of individual rust components in the presence of tannins and phosphoric acid	58
2.6	Corrosion protection via humidity chamber tests and salt spray tests	58
<b>CHAPTER THREE – RESULTS</b>		<b>60</b>
3.1	Tannin extraction	60
3.1.1	Thermogravimetric analysis	63
3.1.2	Prussian blue assay for total phenols in mangrove tannins	66
3.2	Identification of condensed tannins via HPLC analysis	67
3.2.1	Quantification of condensed tannins	78
3.2.1.1	Vanillin assay	78
3.2.1.2	Quantification of flavanoid monomers via HPLC analysis	79
3.3	Anti-oxidant properties of mangrove tannins	80
3.3.1	Reducing power of tannins	80
3.3.2	DPPH and ABTS free radical scavenging activity	81
3.4	Electrochemical tests	83
3.4.1	Inhibition studies of mangrove tannins	83
3.4.1.1	Comparison of the inhibitory action with several commercial tannins	88
3.4.1.2	Synthesis of ferric-tannates	90
3.4.2	Inhibitory performance of catechin, epicatechin, epigallocatechin and epicatechin gallate	96
3.4.2.1	Molecular modelling of flavanoid monomers	103
3.4.3	Cyclic voltammetry	109

3.4.3.1	Redox potential patterns of $1 \times 10^{-3}$ M and $5 \times 10^{-4}$ M catechin	109
3.4.3.2	Redox potential patterns for $1 \times 10^{-3}$ M epicatechin	111
3.4.3.3	Redox potential patterns of tannins	114
3.4.4	Inhibitory performance of mangrove tannins, mimosa tannins and phosphoric acid on pre-rusted steel	119
3.5	Phase transformation studies	124
3.5.1	Phase transformation of rust by tannins	127
3.5.2	Phase transformation of rust in the presence of mangrove tannins and phosphoric acid	134
3.5.3	Phase transformation of the individual rust component in the presence of mangrove tannins	140
3.5.3.1	Interactions of mangrove tannins with lepidocrocite, magnetite, goethite and maghemite via infrared spectroscopy	140
3.5.3.2	Interactions of mangrove tannins with lepidocrocite, magnetite, goethite and maghemite via X-ray diffractions	150
3.5.3.3	Interactions of mangrove tannins with lepidocrocite, magnetite, goethite and maghemite via scanning electron spectroscopy	155
3.5.4	Phase transformation of the individual rust component in the presence of phosphoric acid	158
3.5.5	Evaluation of protective efficiency	165
3.5.5.1	Evaluation of protective efficiency via the humidity chamber tests	165
3.5.5.2	Evaluation of protective efficiency via salt spray tests	171
<b>CHAPTER FOUR – DISCUSSION</b>		<b>174</b>
4.1	Tannin extraction	174
4.1.1	Thermogravimetric analysis	174
4.1.2	Prussian blue assay	175

4.2	Identification of condensed tannins via HPLC analysis	176
4.2.1	Quantification of condensed tannins	179
4.2.1.1	Vanillin assay	179
4.2.1.2	Quantification of flavanoid monomers via HPLC analysis	180
4.3	Anti-oxidant properties of mangrove tannins	182
4.3.1	Reducing power of tannins	182
4.3.2	DPPH and ABTS free radical scavenging activity	183
4.4	Electrochemical tests	185
4.4.1	Inhibition studies of mangrove tannins on clean steel	185
4.4.2	Inhibitory performance of catechin, epicatechin, epigallocatechin and epicatechin gallate	187
4.4.2.1	Molecular modelling of flavanoid monomers	188
4.4.3	Cyclic voltammetry	190
4.4.4	Inhibitory performance of mangrove tannins, mimosa tannins and phosphoric acid on pre-rusted steel	192
4.5	Phase transformation studies	195
4.5.1	Phase transformation of rust by tannins	195
4.5.2	Phase transformation of rust by phosphoric acid and a mixture of mangrove tannins and phosphoric acid	199
4.5.3	Evaluation of protective efficiency by tannins and phosphoric acid	202
	<b>CHAPTER FIVE – CONCLUSION</b>	<b>205</b>
	<b>CHAPTER SIX - FUTURE RESEARCH RECOMMENDATIONS</b>	<b>211</b>
	<b>APPENDICES</b>	<b>213</b>
	<b>REFERENCES</b>	<b>217</b>
	<b>PUBLICATIONS</b>	<b>230</b>



## LISTS OF TABLES

		Page
<b>Table 3.1</b>	IR spectral data of mixed mangrove tannins.	60
<b>Table 3.2</b>	Total phenol content by Prussian blue assay of isolated tannin extracts.	66
<b>Table 3.3</b>	Content of condensed tannins as determined as determined by vanillin assay.	78
<b>Table 3.4</b>	Quantification of flavanoid monomers as determined by HPLC.	79
<b>Table 3.5</b>	Comparison of the inhibition efficiency, <i>IE (%)</i> of steel at pH 0.5 containing the various concentrations of mangrove tannins.	84
<b>Table 3.6</b>	Corrosion potentials of mixed tannins and condensed tannins at different pH values.	86
<b>Table 3.7</b>	Comparison of the inhibition efficiency, <i>IE (%)</i> of steel in HCl at pH 0, 0.5, 2.0 and 4.0 containing 3.0 g L <sup>-1</sup> of the various tannins investigated.	87
<b>Table 3.8</b>	Colour of supernatant and precipitate following centrifugation.	90
<b>Table 3.9</b>	Inhibition efficiency of steel corrosion at different concentrations of flavanoids based on polarisation resistance, <i>R<sub>p</sub></i> measurements at pH 0.5.	102
<b>Table 3.10</b>	Distribution of HOMO electron density of flavanoid molecules.	106
<b>Table 3.11</b>	Total energy, binding energy, heat of formation, total dipole moment, HOMO energies, LUMO energies, HOMO-LUMO energy gap and the fraction electrons transferred from the flavanoid molecule to the iron atom, $\Delta N$ for $\alpha$ electrons calculated from the molecular modelling.	108
<b>Table 3.12</b>	The pH of the flavanoids and tannin solution investigated.	109
<b>Table 3.13</b>	Percentage inhibition of 3.0 g.L <sup>-1</sup> mangrove tannins and mimosa tannins with the addition of 15 %, 30 % and 50 % phosphoric acid in 3.5 % NaCl solution.	119
<b>Table 3.14</b>	Average rust weight of prepared pre-rusted samples.	124

<b>Table 3.15</b>	Principal absorption peaks of the various standard iron oxides.	132
<b>Table 3.16</b>	EDS analysis of pre-rusted samples before and after treatments with 0.5 % mangrove tannins and 15 % phosphoric acid.	139
<b>Table 3.17</b>	EDS analysis of pre-rusted samples before and after treatments with 0.5 % mimosa tannins and 15 % phosphoric acid.	139
<b>Table 3.18</b>	The values of d-spacing for individual rust component.	150
<b>Table 4.1</b>	Half wave potential, $E_{1/2}$ of catechin, epicatechin and tannins.	191
<b>Table 4.2</b>	Transformation of rust components treated with mangrove tannins on samples A, B and C.	196
<b>Table 4.3</b>	Transformation of rust after immersion in phosphoric acid and a mixture of mangrove tannins and phosphoric acid on samples A and C.	199

## LIST OF FIGURES

		Page
<b>Fig. 1.1</b>	(a) Branch tip of <i>Rhizophora apiculata</i> with red stipule and (b) young to old fruits showing the seedlings.	5
<b>Fig. 1.2</b>	Mangrove barks as waste products of the Larut Matang charcoal industry.	5
<b>Fig. 1.3</b>	(a) Gallic acid and (b) hexahydroxydiphenic acid.	7
<b>Fig. 1.4</b>	Classifications of tannins.	8
<b>Fig. 1.5</b>	Structure of a condensed tannin.	9
<b>Fig. 1.6</b>	An example of a Tafel plot.	29
<b>Fig. 1.7</b>	An example of a polarisation resistance curve.	30
<b>Fig. 1.8</b>	Iron-tannate with (a) mono-complex and (b) bis-complexes.	39
<b>Fig. 2.1</b>	A schematic diagram of the extraction of condensed tannins.	43
<b>Fig. 2.2</b>	Three electrode electrochemical cell consisting of platinum counter electrode, KCl saturated calomel electrode and steel working electrode.	51
<b>Fig. 3.1</b>	FTIR spectrum of 70 % aqueous acetone extract (mixed tannins).	61
<b>Fig. 3.2</b>	FTIR spectrum of (a) acetone-water extract and (b) methanol-water extracts following sephadex LH-20 column chromatography.	62
<b>Fig. 3.3</b>	FTIR spectrum of (a) mangrove tannins (b) quebracho tannins (c) mimosa tannins and (d) chestnut tannins.	64
<b>Fig. 3.4</b>	Thermogravimetry analysis (TGA) of mixed tannins, condensed tannins and methanol-water extract.	65
<b>Fig. 3.5</b>	Comparison of the thermogravimetry analysis (TGA) of mangrove tannins with the commercial mimosa, quebracho and chestnut tannins.	65
<b>Fig. 3.6</b>	Chemical structure of flavan-3-ol monomer standards.	70
<b>Fig. 3.7</b>	HPLC chromatogram of flavan-3-ol standards eluted at a flow rate of (a) 1 mL min <sup>-1</sup> and (b) 0.5 mL min <sup>-1</sup> of elution condition (i). Peaks : 1 = (-)-gallocatechin, 2 = (+)-catechin/(-)-catechin, 3 = (-)-epigallocatechin, 4 = (-)-epigallocatechin gallate, 5 = (-)-epicatechin,	

	6 = (-)-gallocatechin gallate, 7 = (-)-epicatechin gallate, 8 = (-)-catechin gallate.	71
<b>FIG. 3.8</b>	HPLC chromatogram of condensed tannins degraded in the presence of acidic dioxane and phloroglucinol.	73
<b>Fig. 3.9</b>	HPLC chromatogram of condensed tannins degraded in the presence of acidic ethanol and phloroglucinol using elution condition (i).	73
<b>Fig. 3.10</b>	HPLC chromatogram of condensed tannins (first sampling) degraded in the presence of acidic ethanol and phloroglucinol using elution condition (ii). Peaks : 1 = phloroglucinol adduct, 2 = catechin, 3=epigallocatechin, 4=epicatechin, 5= epicatechin gallate.	74
<b>Fig. 3.11</b>	HPLC chromatogram of condensed tannins degraded in the presence of acidic ethanol and phloroglucinol spiked with catechin standard. Peaks : 1= phloroglucinol adduct, 2= spiked catechin standard, 3= epigallocatechin, 4= epicatechin.	74
<b>Fig. 3.12</b>	HPLC chromatogram of condensed tannins (second sampling) degraded in the presence of acidic ethanol and phloroglucinol using elution condition (ii). Peaks : 1 = phloroglucinol adduct, 2 = catechin, 3=epigallocatechin, 4=epicatechin, 5= epicatechin gallate.	75
<b>Fig. 3.13</b>	HPLC chromatogram of condensed tannins (second sampling) degraded in the presence of acidic ethanol and phloroglucinol using elution condition (ii). Peaks : 1 = phloroglucinol adduct, 2 = catechin, 3 = spiked epigallocatechin standard, 4 = spiked epicatechin standard, 5 = spiked epicatechin gallate standard.	76
<b>Fig. 3.14</b>	HPLC chromatogram of condensed tannins when spiked with the synthesised adducts of (a) (+)-catechin and (b) (-)-epicatechin. Peaks : 1 = phloroglucinol adduct of condensed sample, 2 = corresponding synthesised catechin/ epicatechin adducts.	76
<b>Fig. 3.15</b>	HPLC chromatogram of the methanol-water extract following degradation reaction in the presence of acidic ethanol and phloroglucinol.	77
<b>Fig. 3.16</b>	The reducing power of tannins as compared to the L-ascorbic and catechin standards.	80
<b>Fig. 3.17</b>	Free radical scavenging activities of tannins measured using DPPH assay. L-ascorbic acid, BHT and catechin were used as reference compounds.	81
<b>Fig. 3.18</b>	Free radical scavenging activities of tannins measured using ABTS assay. L-ascorbic acid and catechin were	

	used as reference compounds.	82
<b>Fig. 3.19</b>	The effect of concentration of mangrove tannins on the potentiodynamic curves of steel at pH 0.5.	83
<b>Fig. 3.20</b>	The effect of concentration of mangrove tannins on the potentiodynamic curves of steel at pH 8.0.	85
<b>Fig. 3.21</b>	The effect of concentration of mangrove tannins on the potentiodynamic curves of steel at pH 0.	86
<b>Fig. 3.22</b>	The potentiodynamic curves of mild steel containing various tannins at pH 0.5.	88
<b>Fig. 3.23</b>	Variation of polarisation resistance, $R_p$ with time of immersion containing 3.0 g L <sup>-1</sup> tannins in HCl solution at pH 4.0.	89
<b>Fig. 3.24</b>	XRD pattern of ferric-tannates synthesised at pH 3.0.	91
<b>Fig. 3.25</b>	UV-visible spectrum of ferric-tannate solution synthesised at several pH following the centrifugation process.	91
<b>Fig. 3.26</b>	FTIR spectrum of (a) mangrove tannins and ferric-tannates synthesised at pH (b) 0.5 (c) 3.0 (d) 4.0 (e) 6.0 and (f) 8.0 after immersion in mangrove tannin solution for 24 hours.	93
<b>Fig. 3.27</b>	FTIR spectrum of (a) mangrove tannins and ferric-tannates after (b) 0.25 hr (c) 1 hour, (d) 7 hours, (e) 24 hours and (f) 48 hours immersion in mangrove tannin solution at pH 3.0.	94
<b>Fig. 3.28</b>	UV spectrums of ferric-tannate solution synthesised at pH 3.0 with respect to time of immersion in mangrove tannin solution.	94
<b>Fig. 3.29</b>	Thermal decomposition profiles of ferric-tannates synthesised at pH 3.0 and pH 8.0.	95
<b>Fig. 3.30</b>	Potentiodynamic curves of steel in HCl at pH 0.5 containing various concentrations of (a) catechin, (b) epicatechin, (c) epicatechin gallate and (d) epigallocatechin.	98
<b>Fig. 3.31</b>	Variation of polarisation resistance, $R_p$ with time of immersion containing (a) 2.5x10 <sup>-3</sup> M, (b) 5.0x10 <sup>-3</sup> M and (c) 1.0x10 <sup>-2</sup> M flavanoids and 2-naphthalene sulfonic acid in HCl at pH 0.5.	100
<b>Fig. 3.32</b>	HOMO density as an isosurface for (a) catechin, (b) epicatechin and (c) epigallocatechin monomers in optimised conformations.	105

<b>Fig. 3.33</b>	Two structural formulas of flavanoids investigated in the molecular modelling experiment.	105
<b>Fig. 3.34</b>	Cyclic voltammograms of $1 \times 10^{-3}$ M catechin at (a) different cycles with a scan rate of $10 \text{ mV s}^{-1}$ , (b) scan rates of $10 - 100 \text{ mV s}^{-1}$ and (c) scan rates of $100 - 1000 \text{ mV s}^{-1}$ .	110
<b>Fig. 3.35</b>	Cyclic voltammograms of $5 \times 10^{-4}$ M catechin at (a) scan rates of $10 - 100 \text{ mV s}^{-1}$ and (b) scan rates of $100 - 1000 \text{ mV s}^{-1}$ .	112
<b>Fig. 3.36</b>	Cyclic voltammograms of $1 \times 10^{-3}$ M epicatechin at (a) scan rates of $10 - 100 \text{ mV s}^{-1}$ and (b) scan rates of $100 - 1000 \text{ mV s}^{-1}$ .	113
<b>Fig. 3.37</b>	Cyclic voltammograms of $3.0 \text{ g L}^{-1}$ mangrove tannins at (a) scan rates of $10 - 100 \text{ mV s}^{-1}$ and (b) scan rates of $100 - 1000 \text{ mV s}^{-1}$ .	115
<b>Fig. 3.38</b>	Cyclic voltammograms of $3.0 \text{ g L}^{-1}$ mimosa tannins at (a) scan rates of $10 - 100 \text{ mV s}^{-1}$ and (b) scan rates of $100 - 1000 \text{ mV s}^{-1}$ .	116
<b>Fig. 3.39</b>	Cyclic voltammograms of $3.0 \text{ g L}^{-1}$ quebracho tannins at (a) scan rates of $10 - 100 \text{ mV s}^{-1}$ and (b) scan rates of $100 - 1000 \text{ mV s}^{-1}$ .	117
<b>Fig. 3.40</b>	Cyclic voltammograms of $3.0 \text{ g L}^{-1}$ chestnut tannins at (a) scan rates of $10 - 100 \text{ mV s}^{-1}$ and (b) scan rates of $100 - 1000 \text{ mV s}^{-1}$ .	118
<b>Fig. 3.41</b>	Potentiodynamic curves of pre-rusted steel containing mangrove tannins and phosphoric acid in 3.5 % NaCl solution at pH 0.5.	120
<b>Fig. 3.42</b>	Variation of polarisation resistance, $R_p$ with time of immersion containing 15 %, 30 % and 50 % phosphoric acid in 3.5 % NaCl solution at pH 2.0.	121
<b>Fig. 3.43</b>	Potentiodynamic curves of pre-rusted steel containing $3.0 \text{ g.L}^{-1}$ mangrove tannins and phosphoric acid in 3.5 % NaCl at pH 5.5.	122
<b>Fig. 3.44</b>	Potentiodynamic curves of pre-rusted steel containing 15 %, 30 %, and 50 % phosphoric acid in 3.5 % NaCl solution at pH 5.5.	123
<b>Fig. 3.45</b>	XRD patterns of rusted surface of sample A with respect to time of immersion : L- lepidocrocite, M- magnetite, X- NaCl.	125
<b>Fig. 3.46</b>	XRD patterns of rusted surface of sample B with respect to time of immersion : L- lepidocrocite,	

	M- magnetite, G-geothite, X- NaCl.	126
<b>Fig. 3.47</b>	SEM micrographs of pre-rusted steel surface before tannin immersion for samples (a) A, (b) B and (c) C and after tannin immersion for samples (d) A, (e) B and (f) C.	128
<b>Fig. 3.48</b>	XRD patterns of rust surface when treated with 0.5 % mangrove tannin for sample A : L- lepidocrocite, M- magnetite, X- NaCl.	129
<b>Fig. 3.49</b>	EDS spectra of (a) rust and (b) tannin treated rust surface for sample A.	130
<b>Fig. 3.50</b>	Phase transformation of bare rust surface when treated with 0.5 % mangrove tannin for (a) sample B and (b) sample C : G-geothite, L- lepidocrocite, M- magnetite.	131
<b>Fig. 3.51</b>	FTIR spectrums of (a) bare rust and (b) converted rust for samples (i) A, (ii) B and (iii) C : FT-ferric-tannate, G-geothite, L-lepidocrocite, M-magnetite.	133
<b>Fig. 3.52</b>	Phase transformation of bare rust surface for sample A immersed in (a) phosphoric acid and (b) 0.5 % mangrove tannin and phosphoric acid solutions : G-geothite, L- lepidocrocite, M- magnetite, V- vivianite, X-NaCl.	135
<b>Fig. 3.53</b>	FTIR spectrum of phosphate and tannate of treated rust for samples (a) A and (b) C : FT-ferric-tannate, P-phosphates, M-magnetite.	136
<b>Fig. 3.54</b>	SEM micrographs of pre-rusted plates for sample A containing (a) 15 % H <sub>3</sub> PO <sub>4</sub> , (b) 15 % H <sub>3</sub> PO <sub>4</sub> and 0.5 % mangrove tannins and (c) 15 % H <sub>3</sub> PO <sub>4</sub> and 0.5 % mimosa tannins and for sample C containing (d) 15 % H <sub>3</sub> PO <sub>4</sub> , (e) 15 % H <sub>3</sub> PO <sub>4</sub> and 0.5 % mangrove tannins and (f) 15 % H <sub>3</sub> PO <sub>4</sub> and 0.5 % mimosa tannins.	138
<b>Fig. 3.55</b>	FTIR spectrum of (i) untreated lepidocrocite and treated with 0.5 % mangrove tannins after (ii) 1 day, (iii) 1 week, (iv) 2 weeks and (v) 1 month immersion : FT-ferric-tannate, L-lepidocrocite.	141
<b>Fig. 3.56</b>	FTIR spectrum of (i) untreated lepidocrocite and treated with 2.0 % mangrove tannins after (ii) 1 day, (iii) 1 week, (iv) 2 weeks and (v) 1 month immersion: FT-ferric-tannate, L-lepidocrocite.	142
<b>Fig. 3.57</b>	FTIR spectrum of (i) untreated magnetite and magnetite treated with 0.5 % mangrove tannins after (ii) 1 day, (iii) 1 week, (iv) 2 weeks and (v) 1 month immersion : FT-ferric-tannate, M-magnetite.	144
<b>Fig. 3.58</b>	FTIR spectrum of (i) untreated magnetite and magnetite	

	treated with 2.0 % mangrove tannins after (ii) 1 day, (iii) 1 week, (iv) 2 weeks and (v) 1 month immersion : FT-ferric-tannate, M-magnetite.	145
<b>Fig. 3.59</b>	FTIR spectrum of (i) untreated goethite and goethite treated with 0.5 % mangrove tannins after (ii) 1 day, (iii) 1 week, (iv) 2 weeks and (v) 1 month immersion : FT-ferric-tannate, G-goethite.	146
<b>Fig. 3.60</b>	FTIR spectrum of (i) untreated goethite and goethite treated with 2.0 % mangrove tannins after (ii) 1 day, (iii) 1 week, (iv) 2 weeks and (v) 1 month immersion : FT-ferric-tannate, G-goethite.	147
<b>Fig. 3.61</b>	FTIR spectrum of (i) untreated maghemite and maghemite treated with 0.5 % mangrove tannins after (ii) 1 day, (iii) 1 week, (iv) 2 weeks and (v) 1 month immersion : FT-ferric-tannate, Mh-maghemite.	148
<b>Fig. 3.62</b>	FTIR spectrum of (i) untreated maghemite and maghemite treated with 2.0 % mangrove tannins after (ii) 1 day, (iii) 1 week, (iv) 2 weeks and (v) 1 month immersion : FT-ferric-tannate, Mh-maghemite.	149
<b>Fig. 3.63</b>	XRD pattern of lepidocrocite treated with (a) 0.5 % and (b) 2.0 % mangrove tannins with respect to time of immersion.	151
<b>Fig. 3.64</b>	XRD pattern of magnetite treated with (a) 0.5 % and (b) 2.0 % mangrove tannins with respect to time of immersion.	152
<b>Fig. 3.65</b>	XRD pattern of goethite treated with (a) 0.5 % and (b) 2.0 % mangrove tannins with respect to time of immersion.	153
<b>Fig. 3.66</b>	XRD pattern of maghemite treated with (a) 0.5 % and (b) 2.0 % mangrove tannins with respect to time of immersion.	154
<b>Fig. 3.67</b>	SEM micrographs of magnetite with two different magnifications.	155
<b>Fig. 3.68</b>	SEM micrographs of (a) untreated magnetite and treated magnetite after (b) one day and (c) 28 days immersion; and (d) untreated lepidocrocite and treated lepidocrocite after (e) one day and (f) 28 days immersion.	156
<b>Fig. 3.69</b>	SEM micrographs of (a) untreated goethite and treated goethite after (b) one day and (c) 28 days immersion; and (d) untreated maghemite and treated maghemite after (e) one day and (f) 28 days immersion.	157
<b>Fig. 3.70</b>	FTIR spectrum of (i) untreated lepidocrocite and lepidocrocite treated with 15 % phosphoric acid after	



	(ii) 1 day, (iii) 1 week, (iv) 2 weeks and (v) 1 month immersion : L-lepidocrocite, P-phosphates.	159
<b>Fig. 3.71</b>	FTIR spectrum of (i) untreated lepidocrocite and lepidocrocite treated with 0.5 % mangrove tannins and 15 % phosphoric acid after (ii) 1 day, (iii) 1 week, (iv) 2 weeks and (v) 1 month immersion : L-lepidocrocite, FT-ferric-tannate, P-phosphates.	161
<b>Fig. 3.72</b>	FTIR spectrum of (i) untreated magnetite and magnetite treated with 0.5 % mangrove tannins and 15 % phosphoric acid after (ii) 1 day, (iii) 1week, (iv) 2 weeks and (v) 1 month immersion : M-magnetite, FT-ferric-tannate, P-phosphates.	162
<b>Fig. 3.73</b>	FTIR spectrum of (i) untreated goethite and goethite treated with 0.5 % mangrove tannins and 15 % phosphoric acid after (ii) 1 day, (iii) 1week, (iv) 2 weeks and (v)1 month immersion : G-goethite, FT-ferric-tannate, P-phosphates.	163
<b>Fig. 3.74</b>	FTIR spectrum of (i) untreated maghemite and maghemite treated with 0.5 % mangrove tannins and 15 % phosphoric acid after (ii) 1 day, (iii) 1 week, (iv) 2 weeks and (v) 1 month immersion : Mh-maghemite, FT-ferric-tannate, P-phosphates.	164
<b>Fig. 3.75</b>	Evolution of rust formation with time for pre-rusted samples treated with 0.5 % mangrove tannins.	166
<b>Fig. 3.76</b>	Evolution of rust formation with time for pre-rusted samples treated with 0.5 % mimosa tannins.	167
<b>Fig. 3.77</b>	Evolution of rust formation with time for pre-rusted samples treated with 15 % phosphoric acid.	168
<b>Fig. 3.78</b>	Evolution of rust formation with time for pre-rusted samples treated with 0.5 % mangrove tannins and 15 % phosphoric acid.	169
<b>Fig. 3.79</b>	Evolution of rust formation with time for pre-rusted samples treated with 0.5 % mimosa tannins and 15 % phosphoric acid.	170
<b>Fig. 3.80</b>	Rusted plate after six hours of exposure in the salt spray chamber.	171
<b>Fig. 3.81</b>	Evolution of rust formation of pre-rusted plates immersed in (a) 0.5 % mangrove tannins, (b) 0.5 mimosa tannins, (c) 15 % phosphoric acid, (d) 0.5 % mangrove tannins and 15 % phosphoric acid and (e) 0.5 % mimosa tannins and 15 % phosphoric acid.	173
<b>Fig. 4.1</b>	Acid depolymerisation of condensed tannins in the presence of phloroglucinol. "ACB" and "DFE" represents	

	extender and terminal units respectively. $R_1, R_3=OH$ and $R_2, R_4=H$ for pyrocatechol; $R_1, R_3=OH$ and $R_2, R_4=OH$ for pyrogallol.	176
<b>Fig. 4.2</b>	Chemical structure of flavanoid monomers that constitute mangrove tannins.	178
<b>Fig. 4.3</b>	Chemistry of the vanillin assay for condensed tannins.	179
<b>Fig. 4.4</b>	Suggested structure for the ferric-tannate formed from mangrove tannins with catechin representing the monomer unit.	187
<b>Fig. 4.5</b>	Proposed mechanism of catechin in AAPH radical oxidation.	190
<b>Fig. 4.6</b>	Profile of the transformation of rust into ferric-tannates.	196

## LIST OF ABBREVIATIONS

FTIR	Fourier transform infrared spectroscopy
TGA	Thermogravimetric analysis
DTG	Differential thermogravimetric
NMR	Nuclear magnetic resonance
XRD	X-ray diffraction
SEM	Scanning electron microscopy
EDS	Electron dispersive X-ray spectroscopy
HOMO	Highest occupied molecular orbitals
LUMO	Lowest unoccupied molecular orbitals
SHE	Standard hydrogen electrode
$I_{corr}$	Corrosion current
$E_{corr}$	Corrosion potential
$R_p$	Polarisation resistance
wt	weight
v	volume
w/v	weight per volume
min	minutes
hr	hour
ha	hectar
$\text{g L}^{-1}$	gram per liter
$\text{mg mL}^{-1}$	milligram per millilitre
$\text{mL min}^{-1}$	milliliter per minute
mV	millivolts
$\text{mV s}^{-1}$	millivolt per second
$\mu\text{A}$	microampere

br	broad
s	strong
m	medium
w	weak

## PHYSICO-CHEMICAL CHARACTERISATION OF MANGROVE TANNINS AS CORROSION INHIBITORS

### ABSTRACT

Tannins from mangrove barks have been successfully extracted using 70 % aqueous acetone and purification by LH-20 column chromatography afforded condensed tannins of high purity. The reversed-phase HPLC analysis of condensed tannins following depolymerisation in phloroglucinol and acidic ethanol revealed mainly four terminal units namely catechin, epicatechin, epigallocatechin and epicatechin gallate. Substantial anti-oxidant capabilities have been shown by mangrove tannins which were comparable to the synthetic standards used.

The electrochemical experiments have shown that the inhibitive efficiency of mangrove tannins on steel which was largely contributed by the condensed tannins, increased with increasing concentrations at very low pH. The inhibitive performance of mangrove tannins was comparable with that of commercial mimosa, quebracho and chestnut tannins at pH 0, 0.5 and 2.0. All tannins that were investigated are cathodic inhibitors in acidic media and the inhibition efficiency of all tannins was found to decrease with increasing pH. At pH 0 and 0.5 the adsorption mechanism was attributed to chemisorption of tannin molecules onto the iron surface while at higher pH, the formation of ferric-tannates resulted in a low protective effect. The electrochemical studies have shown that the flavanoid monomers that constitute mangrove tannins are potential inhibitors for steel in acidic medium. All monomers act mainly as cathodic inhibitors of the steel corrosion and its inhibitive performance

dependent on concentration in acidic conditions. To explain the adsorptive behaviour of the molecules on the steel surface, a semi-empirical approach involving quantum chemical calculations using HyperChem 6.0 was undertaken. The correlation between the electronic density of the molecule and the inhibiting properties was established. The most probable adsorption centers were found in the vicinity of the phenolic groups.

Inhibition efficiency of pre-rusted steel in 3.5 % NaCl solution containing 3.0 g L<sup>-1</sup> tannins was found to be dependent on the concentration of phosphoric acid added and pH of solution. The correlation between ferric-tannate formation and the low inhibition efficiency observed at high pH from the electrochemical studies was established from phase transformation studies, evaluated via FTIR, XRD, SEM, EDS, humidity chamber and salt spray tests. All methods of evaluation inferred a temporary and low corrosion protection by mangrove tannins.

## **PENCIRIAN FISIKOKIMIA TANIN BAKAU SEBAGAI PERENCAT KAKISAN**

### **ABSTRAK**

Tanin daripada kulit kayu bakau telah diekstrak menggunakan 70 % aseton akueus dan penulenan tanin menggunakan kromatografi turus LH-20 menghasilkan tanin terkondensasi yang bertulenan tinggi. Analisis HPLC fasa berbalik selepas proses pendepolimeran dalam floroglusinol beralkohol menghasilkan empat unit penghujung iaitu katecin, epikatecin, epigallokatecin dan epikatecin gallat. Tanin bakau turut menunjukkan keupayaan anti-oksidan yang setanding dengan bahan piawai sintetik yang digunakan.

Kajian elektrokimia menunjukkan bahawa keupayaan perencatan terhadap keluli yang sebahagian besarnya disumbang oleh tanin terkondensasi, bertambah dengan peningkatan kepekatannya pada pH rendah. Keupayaan perencatan tanin bakau adalah setanding tanin mimosa, quebracho dan chestnut pada pH 0, 0.5 dan 2.0. Kesemua tanin yang diselidik adalah perencat katodik dalam media berasid yang mana keupayaan perencatannya berkurang dengan peningkatan pH. Pada pH 0 dan 0.5, mekanisme perencatan adalah oleh proses pengkimierapan molekul tanin ke atas permukaan besi manakala pada pH yang lebih tinggi, pembentukan ferik-tanat memberikan perlindungan kakisan yang rendah. Kajian elektrokimia juga telah menunjukkan monomer flavanoid yang terkandung dalam tanin bakau berpotensi bertindak sebagai agen perencat kakisan terhadap keluli pada media berasid. Kesemua monomer flavanoid yang dikaji adalah perencat katodik dan keupayaan perencatan kakisan adalah bergantung pada kepekatan dalam media berasid. Untuk

menerangkan sifat penjerapan molekul ke atas keluli, pendekatan pengiraan kuantum kimia menggunakan Hyperchem 6.0 dijalankan. Korelasi antara ketumpatan elektron dan sifat perencatan kakisan dikenalpasti. Kajian menunjukkan penjerapan tertumpu pada kumpulan fenol. Keupayaan perencatan terhadap kakisan keluli dalam 3.5 % larutan NaCl yang mengandungi  $3.0 \text{ g L}^{-1}$  tanin bergantung pada kepekatan asid fosforik dan pH larutan. Korelasi antara pembentukan ferik-tanat dan keupayaan perencatan rendah yang ditunjukkan oleh kajian elektrokimia dikenalpasti melalui kajian perubahan fasa yang dinilai melalui kaedah FTIR, XRD, SEM, EDS, ujian kelembapan dan semburan garam. Kesemua kaedah penilaian menunjukkan tanin bakau memberikan perlindungan yang rendah dan bersifat sementara terhadap kakisan.



# CARACTÉRISATION ÉLECTROCHIMIQUE DES TANNINS DE LA MANGROVE EN TANT QU'INHIBITEURS DE CORROSION

## RÉSUMÉ

Des tannins ont pu être extraits avec succès des écorces de mangrove grâce à une solution aqueuse d'acétone à 70 % et leur purification par chromatographie sur colonne LH-20 a permis d'obtenir des tannins condensés très purs. L'analyse des tannins condensés par HPLC à polarité de phase inversée, après dépolymérisation dans le phloroglucinol et l'éthanol acide, a révélé l'existence de quatre unités terminales principales, à savoir la catéchine, l'épicatéchine, l'épigallocatechine et l'épicatéchine gallate. Ces tannins de mangrove ont montré des capacités anti-oxydantes importantes, comparables aux standards synthétiques utilisés.

Les expériences électrochimiques ont démontré que l'efficacité inhibitrice de corrosion des tannins de mangrove sur l'acier, due en grande partie à la présence des tannins condensés, croît avec leur concentration à très bas pH. Leur capacité inhibitrice s'est avérée comparable à celle des tannins commerciaux de mimosa, de québracho et de châtaignier à pH 0, 0,5 et 2,0. Tous les tannins étudiés sont des inhibiteurs cathodiques en milieu acide et, pour tous, l'efficacité d'inhibition diminue lorsque le pH augmente. A pH 0 et 0,5, le mécanisme d'adsorption a été attribué à la chimisorption des molécules de tannin sur la surface du fer, alors qu'à pH plus élevé, la formation de tannates ferriques a conduit à un faible effet protecteur. Les études électrochimiques menées ont également démontré que les monomères flavanoïdes qui constituent les tannins de la mangrove sont en eux-mêmes des

inhibiteurs potentiels pour l'acier en milieu acide. Tout comme les tannins de mangrove, les monomères agissent principalement comme des inhibiteurs cathodiques de la corrosion de l'acier et leurs performances inhibitrices dépendent de leur concentration en milieu acide.

Afin d'expliquer le comportement d'adsorption des molécules sur la surface de l'acier, une approche semi-empirique, impliquant des calculs de chimie quantique et utilisant HyperChem 6.0, a été adoptée. Ainsi, nous avons pu établir une corrélation entre la densité électronique de la molécule et les propriétés inhibitrices. Les centres d'adsorption les plus probables se situent dans le voisinage des groupes phénoliques.

D'autre part, l'efficacité d'inhibition de la corrosion sur des échantillons d'acier pré-rouillés, observée dans une solution de NaCl à 3,5 % contenant  $3 \text{ g L}^{-1}$  de tannins, est apparue dépendante de la concentration d'acide phosphorique ajouté et du pH de la solution. La corrélation entre la formation de tannates ferriques et la faible efficacité d'inhibition observée à pH élevé lors des études électrochimiques a été confirmée par (l'observation de transformations de phases réalisée par à enlever) des analyses IRTF, DRX, MEB, EDS et des tests en enceinte humidotherme et en brouillard salin. Toutes les méthodes d'évaluation ont permis de conclure à une protection contre la corrosion par les tannins de mangrove faible et temporaire.

# CHAPTER ONE

## INTRODUCTION

### 1.1 Mangrove forests in Malaysia

Mangrove forests in Malaysia develop well in sheltered estuaries where waters are brackish, and wave and tidal conditions are conducive to mud accumulation. In total, there are about 641,000 ha of mangrove forests in Malaysia of which 57 % are found in Sabah, 26 % in Sarawak and the remaining 17 % in peninsular Malaysia. Of the total, about 446,000 ha or 70 % have been gazetted as forest reserves. Currently, there are a total of 112 mangrove forest reserves in the country. These reserves form part of the country's Permanent Forest Estate which is managed for sustainable forestry production.

In peninsular Malaysia, the total extent of mangrove forests is about 107,700 ha. About 92,300 ha (85.7 %) are forest reserves while the remaining 15,400 ha (14.3 %) are stateland mangroves. Amongst the 11 states in Peninsular Malaysia, Perak has the greatest number of mangrove reserves of which 19 reserves form the Matang mangroves (Clough, 1993).

Traditionally, mangroves are harvested for fuel (as firewood or first converted to charcoal) and for poles (now mainly used as piling). Species of the family Rhizophoraceae, mainly *Rhizophora apiculata*, *R. mucronata* and *Bruguiera parviflora* are particularly favoured for making charcoal because of their hard, dense timber, claimed by some to produce the best charcoal in the world. In the

Matang mangroves in the State of Perak, we see what is considered to be the best managed mangrove forest in the world (Gan, 1995). The Matang mangroves are a large expanse of mangrove forest (about 51km of coastline and 13km wide) stretching from Kuala Gula in the north to Bagan Panchor in the south. It represents the largest intact tract of mangrove forest with several semi-permanent lakes in Peninsular Malaysia and one of the last mangrove areas with all major habitats and forest types.

The main vegetation types of Matang (Silvius *et al.*, 1986) are :

- “Bakau type” (*Rhizophora* spp.). More than 80 % of the mangroves are mainly *R. apiculata* due to reforestation;
- “Api api-Perapat” type (*Avicennia-Sonneratia*). This type occurs mainly in the accreting mangrove zone. In some areas, *Avicennia* covers large areas of forest;
- “Berus type” (*Bruguiera cylindrica*), which occurs close to the coast mostly behind the *Avicennia-Sonneratia* type;
- “Lenggadai type” (*B. parviflora*); and
- “Tumu type” (*B. gymnorhiza*), which is the climax mangrove forest type, preceding the inland forest.

With a total of about 41,000 ha of managed forest, 1,000-1,300 ha of the Matang mangroves are now cut annually on a 30 year rotation. Two thinning are carried out, the first at 15 years and the second at 20 years. Poles cut during thinning are used for construction, and in some cases for firewood. Gross revenue from charcoal and other products has been estimated at about US\$6

million. Extraction and processing of timber from the Matang mangrove forest has been estimated to provide employment for a direct workforce of about 1,400 people and an indirect workforce of a further 1,000 (Clough,1993).

However, due to forest harvesting, the major part of the forest is not higher than 10-20 m. The soil is basically mixed with a high percentage of clay, varies from compact blue clay, containing little or no organic matter, in the more recent deposits on the sea face, to the brown “mangrove loam”, with a high proportion of partly decomposed organic matter and a varying amount of sand, in the centre of the islands and along the mainland boundary (Gan,1995).

#### **1.1.1 *Rhizophora* in general (Family-Rhizophoraceae)**

All *Rhizophora* species have arching stilt roots that emerge from the trunk, hence their scientific name *Rhizophora* which means "root bearer" in Greek. These roots not only hold up the tree in soft mud, but are also permeable to gases, while remaining impermeable to salts. The entire upper root system including the trunk and prop roots that emerge from the branches have this feature. Thus the roots also help the tree to breathe. *Rhizophora* use ultrafiltration at the root level to exclude salt. It is believed that they store any salt that gets through in old leaves which they later shed. *Rhizophora* grow best in wet, muddy and silty sediments.

The tiny flowers are wind-pollinated, producing lots of powdery pollen and no fragrance or nectar. They are also self-pollinating. The fruit does not fall away when it ripens. Instead, the single seed within the fruit starts to germinate while

it is still on the mother tree, and the mother tree channels nutrients to the growing seedling (vivipary). The seedling forms a stem (called a hypocotyl). When the seedling finally falls, at first it floats horizontally, and drifts with the tide. It can survive for long periods at sea. After some weeks, the tip gradually absorbs water and the seedling floats vertically and starts to sprout its first leaf from the top, and roots from the bottom. When it hits land, it grows more roots to anchor itself upright, and then more leaves. *Rhizophora* seedlings grow rapidly to avoid being submerged at high tide. They can grow by 60cm in the first year. Because *Rhizophora* are fast growing and flower within their first year, they are often used to replant mangroves either for conservation or as part of a managed forest to produce timber for construction or charcoal (Tan, 2001).

### **1.1.2 *Rhizophora apiculata* (bakau minyak)**

The commonly found mangrove species within the *Rhizophora* genus are *Rhizophora mucronata*, *Rhizophora stylosa*, *Rhizophora mangle* and *Rhizophora apiculata*. The *Rhizophora apiculata* tree can reach up to 20 m tall. It has elliptic leaf blades with tiny black spots below the leaf blades, with red stipules and the leaf stalks are often tinged red. The paired stalkless flowers are cream-coloured sitted on a short, stout dark grey stalk. Its fruits are pear-shaped and brown in colour (Fig. 1.1). Although *Rhizophora apiculata* have been used mainly for charcoal making, leaving the barks (Fig. 1.2) as waste products, Mohd. Ali *et al.*, (1981) reported that the 10% tannin content extracted from the barks of *Rhizophora apiculata* was sufficient for commercial exploitation.



(a)



(b)

**Fig. 1.1** (a) Branch tip of *Rhizophora apiculata* with red stipule and (b) young to old fruits showing the seedling (Ng and Sivasothi, 2001).



**Fig. 1.2** Mangrove barks as waste products of the Larut Matang charcoal industry.

## 1.2 What are tannins?

The name 'tannin' is derived from the French 'tanin' (tanning substance) and is used for a range of natural polyphenols. Since ancient times it is known that certain organic substances have tanning properties and are able to tan animal skins to form leather. In nature the tannins are found worldwide in many different families of the higher plants such as in chestnut, pine and oak wood, depending on their origin, their chemistry varies widely, having a molar mass of up to 20,000D. High tannin concentrations are found in nearly every part of the plant, such as in the bark, wood, leaves, fruit, roots and seed.

The nomenclature of the tannins is full of misunderstanding, erroneous interpretations, and changes caused by advances in this field. Definitions include the plant tannins as water soluble phenolic compounds with a molar mass between 300 and 3,000, showing the usual phenol reactions (e.g. blue colour with iron (III) chloride and precipitating alkaloids, gelatine and other proteins (Bates-Smith and Swain,1962) tannins with a molecular weight that can reach 5000, contain sufficient phenolic hydroxyl groups to permit the formation of stable cross-links with proteins, and as a result cross-linking enzymes may be inhibited (Ximenes,1998) and tannins have also been described as oligomeric compounds with multiple structure units with free phenolic groups, having molecular weight ranging from 500 to >20,000 and soluble in water with the exception of some high molecular weight structures (Tannins : Chemical Structure, 2001). Tannins were classified into two broad groups: the hydrolysable and condensed tannins (Okuda *et al.*,1989). Gallic acid [Fig.1.3(a)] and hexahydroxydephinic acid with HHDP group [Fig.1.3(b)] represent the



polyphenolic part in the molecules of hydrolysable tannins as a result of their hydrolysis and condensation in the presence of acid and enzyme. Those having the HHDP group have been named ellagitannins as they produce ellagic acid upon hydrolysis and those having only the galloyl groups are called gallotannin.

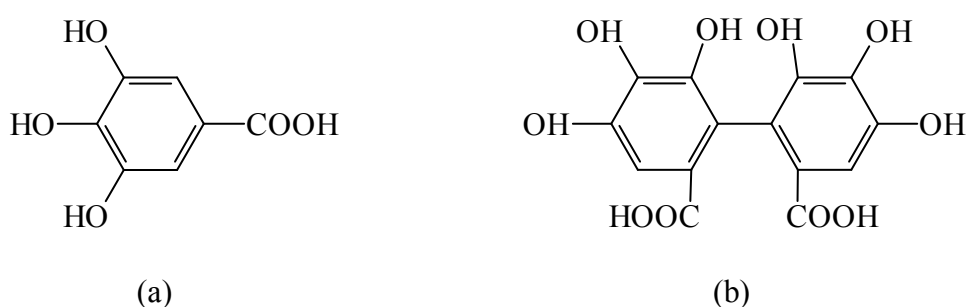


**Fig. 1.3** (a) Gallic acid and (b) hexahydroxydiphenic acid.

However, based on the molecular structures of the currently known tannins, their origin and role in plant life, Khanbabae and Van Ree (2001) suggested that tannins be divided into four major groups : *Gallotannins*, *ellagitannins*, *complex tannins* and *condensed tannins* (Fig. 1.4).

- (1) Gallotannins are all those tannins in which galloyl units or their *meta*-depsidic derivatives are bound to diverse polyol-, catechin-, or triterpenoid units.
- (2) Ellagitannins are those tannins in which at least two galloyl units are C-C coupled to each other, and do not contain a glycosidically linked catechin unit.

(3) Complex tannins are tannins in which a catechin unit is bound glycosidically to a gallotannin or an ellagitannin unit.

(4) Condensed tannins are all oligomeric and polymeric proanthocyanidins formed by linkage of C-4 of one catechin with C-8 or C-6 of the next monomeric catechin (Khanbabaee and Van Ree, 2001).

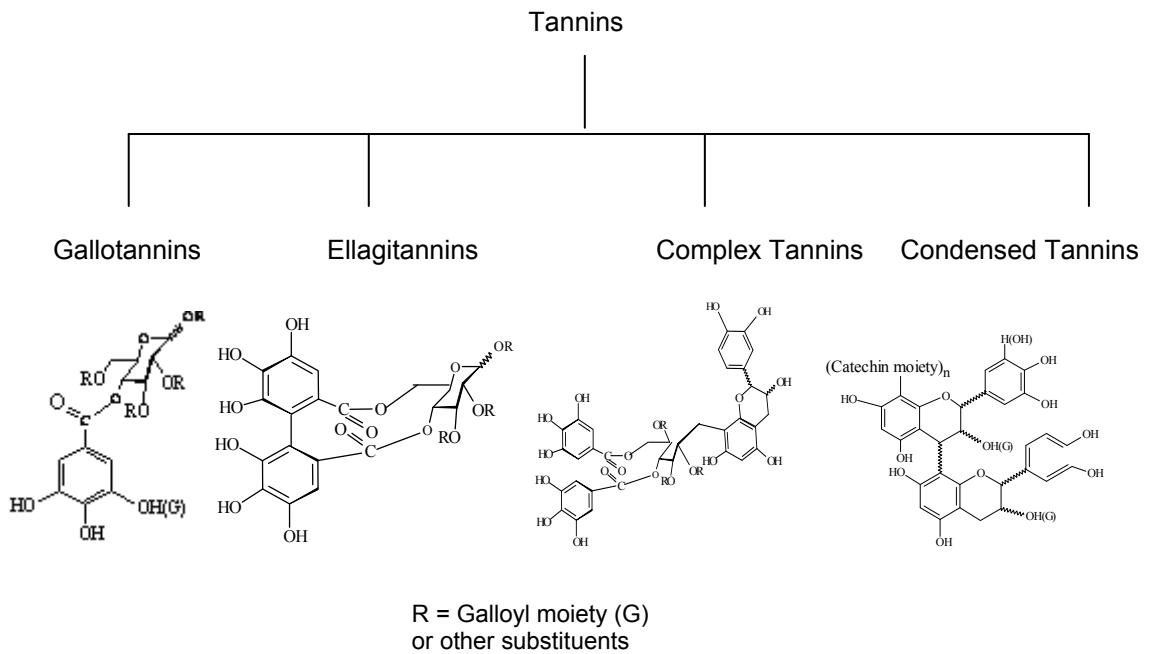


**Fig. 1.4** Classifications of tannins (Khanbabaee and Van Ree, 2001).

### 1.2.1 Condensed tannins (or proanthocyanidins)

Proanthocyanidins (condensed tannins) are a group of phenolic polymers which are widely distributed in the plant kingdom particularly with woody growth habit. These compounds consist of flavan-3-ol units linked together through C4-C6 or C4-C8 bonds (Fig.1.5). Structural variation of proanthocyanidins ranges from dimers and trimers to more complex oligomers and polymers depending on the nature of the interflavanoid linkage, hydroxylation and stereochemistry at the three chiral centres (carbon 2, 3 and 4) of the C-ring. They are the most widespread polyphenols in plants after lignins and can be found in leaves, fruit woods, barks or roots and are known to play various nutritional and ecological roles [Farreira *et al.* (1999) and other authors therein].

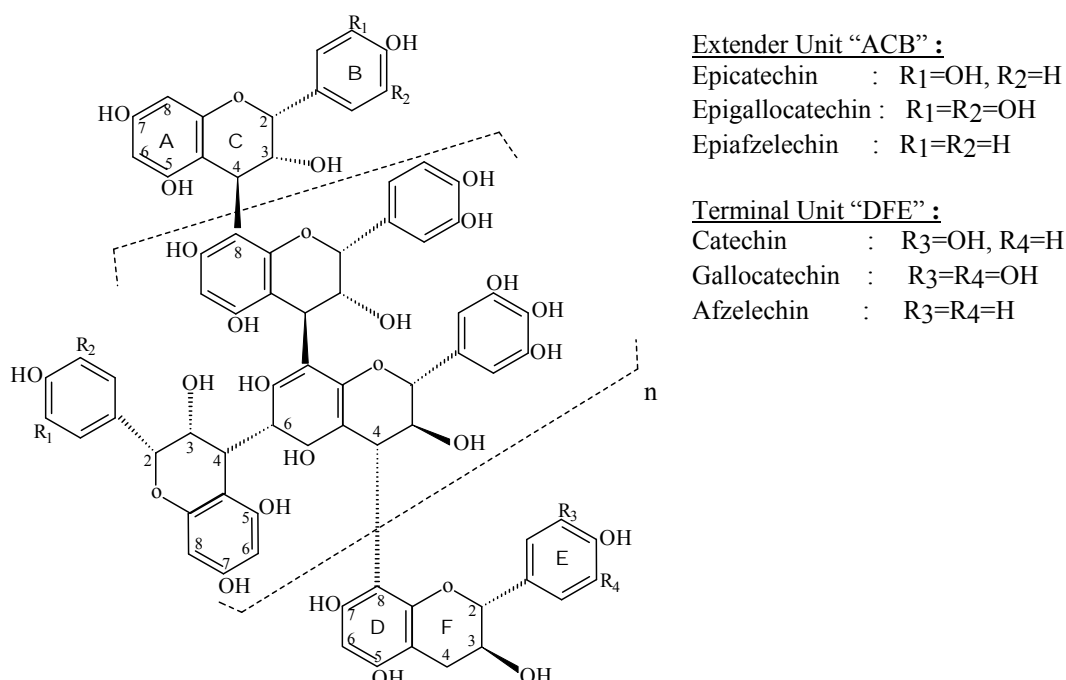


**Fig. 1.5** Structure of a condensed tannin (Hernes *et al.*, 2001).

These flavan-3-ol oligomers produce anthocyanidins by cleavage of a C-C bond under strongly acidic conditions. The most important features of the flavan-3-ols pertaining to the chemistry of oligomeric proanthocyanidins are the nucleophilicity of the A-rings, the aptitude of their heterocyclic rings to cleavage and subsequent rearrangement, the susceptibility of analogues with pyrocatechol- or pyrogallol-type B-rings to phenol oxidative coupling, and the conformational mobility of their pyran rings (Farreira *et al.*, 1999). With the growing realization of the importance of these compounds as antioxidants in the human diet, this has led to a sharp increase in research effort. Extensive studies were carried out on the isolation and characterization of condensed tannins from various plant sources mainly by using NMR techniques (Karchesy and Hemingway, 1980; Porter *et al.*, 1982; Marimoto *et al.*, 1986; Kashiwada *et al.*, 1986; Ishimatsu *et al.*, 1989; Cai *et al.*, 1991; Toki *et al.*, 1991; Danne *et al.*, 1993; Nam-In *et al.*, 1994) and HPLC analysis (Da Silva, 1991; Rigaud *et al.*, 1993; Prieur *et al.*, 1994; Jean-Marc *et al.*, 1996; Guyot *et al.*, 1997; Hammerstone *et al.*, 1999) as well as TLC techniques (Porter *et al.*, 1985; Foo and Karchesy, 1991; Kolodziej *et al.*, 1991; Young-Soo *et al.*, 1994). The review that follows demonstrates that, although considerable progress has been made in definition of proanthocyanidin structure, understanding of the properties of these complex compounds is still rather limited.

### 1.2.1.1 Analysis of condensed tannins

Analysis of condensed tannins is complicated by the diversity of structures found within this group of compound. Many analytical methods have been used to quantify condensed tannins in plant materials. Commonly used methods include the vanillin assay (Price *et al.* 1978; Makkar and Becker, 1994; Naczek *et al.*, 1994) and oxidative depolymerization reactions such as the acid-butanol assay (Hagerman and Butler 1988; Makkar *et al.*, 1999). Other methods involve protein precipitation reactions (Makkar, 1989), Stiasny reaction (Yazaki, 1985), acid cleavage reactions, enzyme and microbial inhibition and gravimetric procedures (Schofield *et al.*, 2001). A more recent addition to the list of analysis is the use of flow injection spectrophotometry (Ferreira and Nogueira, 2000). An excellent review with regard to the most appropriate procedures to choose for a sample is given by Schofield *et al.* (2001).

Depolymerisation reactions in the presence of nucleophiles are frequently employed for the structural analysis of proanthocyanidins. The nucleophile forms adducts with the extender units in the polymer, which are purified or analysed by chromatography. Their structure, once established, can be used to determine the nature of the monomer units within the polymer. Numerous nucleophiles have been used including benzylthiol (Foo and Karchesy, 1991), benzyl mercaptan (Guyot *et al.*, 1997; Matthews *et al.*, 1997) or phloroglucinol (Brandon *et al.*, 1989; Koupai-Abyazani *et al.*, 1992; Prieur *et al.*, 1994; Achmadi *et al.*, 1994). Depolymerisation in the presence of a nucleophile offers several advantages. Associated with the quantitative analysis of the products by

chromatography, it may simultaneously offer information on the nature of the proanthocyanidins. In contrast to colorimetric methods, interferences with other plant constituents are avoided due to the nonambiguous identification of the proanthocyanidin-derived products. In comparison to the butanol/HCl depolymerisation, the reaction preserves the stereochemistry at the C2-C3 positions of the polymer units. The use of a nucleophile limits the occurrence of side reactions that could affect recovery yields of the products (Matthew *et al.*, 1997).

### **1.2.2 Uses of tannins**

The tannins are applied widely, with uses ranging from tanning, known over millennia (since *ca.* 1500 BC), through medical uses to uses in the food industry. The biological significance (e.g. protection of plant from insects, diseases and herbivores) and current uses (e.g. leather manufacture) and promising new uses (e.g. as pharmaceuticals and wood preservatives) of tannin rest on their complexation with other biopolymers (e.g. proteins and carbohydrates, or metal ions) (Farreira *et al.*, 1999). The structure, stereochemistry and reactivity of some natural condensed tannins have been described in detail by Roux *et al.* (1975).

Leather tanning industry is one of the most ancient industries known. Although the technology of leather has evolved over the years, the basic principles for the production of leather have remained the same. Hide proteins, mainly collagen, are rendered insoluble and dimensionally more stable by treatment with

chemical products such as natural vegetable tannins so as to produce leather which is more resistant to mechanical wear and less susceptible to biological and other types of attack. In view of the continuing interests in producing quality leathers, a new formulation of sulfonated melamin-urea-formaldehyde resin containing different vegetable tannins which is able to produce leather with the same good characteristics of leather prepared with chrome salts has been developed (Simon and Pizzi, 2003). In addition Pizzi *et al.* (2004) have established the correlation between the antioxidant capability of tannins and the problem of colour variation of leather.

Tannins as adhesives perhaps are the second most important bulk use other than for leather. Their use as wood adhesives is based mainly on the reaction, gelling and hardening of these tannins and formaldehyde (Fechtal and Riedl, 1993). Recent studies on tannin-based adhesives have included rheological studies of various tannin extracts (Garnier *et al.*, 2001; Garnier *et al.*, a,b, 2002), the building of time-temperature-transformation curing diagrams for the understanding of the behaviour of thermosetting resins under isothermal cure conditions and continuous heating transformation (Garnier and Pizzi, 2001), condensed tannin of Douglas-fir and polyethylenimine as formaldehyde-free wood adhesives (Li *et al.*, 2004) and bonding quality of *Eucalyptus globulus* plywood using tannin-phenol-formaldehyde adhesives (Vazquez *et al.*, 2003).

Following the realisation that a wide range of herbal medicines and foodstuffs may be credited for preventive effects on chronic diseases due to their radical scavenging activities or antioxidant properties, increasing attention has been

directed to the development of safe and effective functional foods and extraction of novel antioxidants from medicinal plants (Latté and Kolodziej, 2004). Indeed the radical scavenging activities or antioxidant capabilities of tannins have been confirmed by several authors evaluated by colorimetry (Minussi *et al.*, 2003; Gulcin *et al.*, 2003; Goh *et al.*, 2003; Mi-Yea *et al.*, 2003; Cakir *et al.*, 2003; Nessa *et al.*, 2004), electron spin resonance (ESR) techniques (Noferi *et al.*, 1997; Fedeli *et al.*, 2004), chemiluminescence (CL) techniques (Ohtani *et al.*, 2000; Latté and Kolodziej, 2004) and Rancimat and Oxidograph tests (Lampart-Szczapa *et al.*, 2003). An overview on the biological activities of proanthocyanidins as regards to its antimicrobial and antiviral properties, enzyme-inhibiting properties, mutagenicity, antimutagenicity and antitumoral activity and antioxidative properties have also been summarised (De Bruyne *et al.*, 1999).

Recent development of the industrial uses of tannins as corrosion inhibitors in the formulations of pigments in paint coatings (Foster *et al.*, 1991; Matamala *et al.*, 1994; Batis *et al.*, 1997; Clough, 1997; Pardini *et al.*, 2001), flocculants (Kelly *et al.*, 1988; Meyer and Woods, 1993; Lamb and Decusati, 2002;) depressants (Bulatovic and Salter, 1989), viscosity modifier agent, chemical cleaning agents for removing iron-based deposits (AL-Mayauf, 1997) and oxygen scavengers for boiler water treatment system (Sato *et al.*, 1990; Yoshiaki and Toshinobu, 1994) reflects their importance as industrial raw materials relative to the synthetic phenols.



### **1.3 Corrosion inhibitors**

In many industries, the need to use constructional materials safely, but cost-effectively, is a primary consideration. Frequently, physical requirements can be satisfied easily, but corrosion effects seriously complicate the selection of suitable materials. Generally, increased corrosion-resistance can only be obtained at increased cost. However, the actual material-related costs incurred in a project will depend on the corrosivity of the environment concerned, the required design life, the physical requirements of the material, and the readily available stocks. In some cases, appearance may also dictate the use of a more expensive material. The costs and problems associated with corrosion-resistant materials means that, in many cases, the use of corrosion inhibitors is a practical and economic alternative. Industrial use of corrosion inhibitors is, therefore, now broad based and extensive.

#### **1.3.1 Classification of corrosion inhibitors**

At the simplest level, a corrosion inhibitor is a substance which when added in small concentration to an environment effectively reduces the corrosion rate of a metal exposed to that environment. Scientifically, exacting definition is really not possible in general sense where mechanistic and/or chemical considerations serve to sub-divide corrosion inhibitors into specific types or classes.

Classification of corrosion inhibitors is somewhat a subjective exercise being very much dependent on the mechanism employed. For example, one could

choose to classify in terms of mechanism and environment to which they are added. Inhibitor such as 2,5-bis(3-pyridyl)-1,3,4-thiadiazole (El Azhar *et al.*, 2002) is categorised as an anodic inhibitor, 2-naphthalene sulfonic acid (Vracar and Drazic, 2002) and salicylic acid hydrazide (Quraishi *et al.*, 2001) as cathodic inhibitors while mercapto-triazole derivatives (Wang *et al.*, 2004), 2-mercaptobenzoimidazole (Morales-Gil *et al.*, 2004), benzoic acid hydrazide (Quraishi *et al.*, 2001), diazoles (Popova *et al.*, 2003), L-ascorbic acid (Ferreira *et al.*, 2004) and triphenyl phosphonium chloride (Khaled, 2004) are mixed type inhibitors. These categorisations however are dependent on the metals, type and concentrations of the corrosion medium under study. For example 3,5-bis(4-methylthiophenyl)-4H-1,2,4-triazole on mild steel is a mixed type inhibitor in 1 M HCl and a cathodic inhibitor in 0.5 M H<sub>2</sub>SO<sub>4</sub> (Lagrene *et al.*, 2002).

### **1.3.2 Effects of corrosion inhibitors on corrosion processes**

Studies have shown that the efficiency of inhibition can be qualitatively related to the amount of adsorbed inhibitor on the metal surface. The adsorption of inhibitors is governed by the residual charge on the surface of the metal and by the nature and chemical structure of the inhibitor. The two main types of adsorption of an inhibitor on a metal surface are physical or electrostatic and chemisorption. Adsorption isotherms are often used to demonstrate the performance of adsorbent-type inhibitors. The adsorption of several inhibitors have been described by Langmuir (El Azhar *et al.*, 2002; Morales-Gil *et al.*, 2004; Hui-Long *et al.*, 2004), Temkin (Quraishi *et al.*, 2001; Hosseini *et al.*,

2003; Lgamri *et al.*, 2003; Khaled, 2004) and Frumkin (Vracar and Drazic, 2002; Popova *et al.*, 2003) adsorption isotherms.

Physical adsorption is due to the electrostatic attraction between the inhibiting ions or dipoles and the electrically charged surface of the metal. The forces in the electrostatic adsorption are generally weak. The inhibiting species adsorbed on the metal due to electrostatic forces can also be desorbed easily. A main feature of electrostatic adsorption is that the ions are not in direct physical contact with the metal. A layer of water molecules separates the metal from the ions. The physical adsorption process has a low activation energy and is relatively independent of temperature (Mansfield, 1987a).

Chemisorption is probably the most important type of interaction between the metal surfaces and an inhibitor molecule in corrosion inhibition systems. The adsorbed species is in contact with the metal surface. The chemisorption process is slower than electrostatic sorption and has higher activation energy. The temperature dependency shows higher inhibition efficiencies at higher temperatures. Unlike electrostatic adsorption, it is specific for certain metals and is not completely reversible. Adsorption results from polar or charged nature of the organic molecule/ionic species first establishing a physisorbed surface film (through Van der Waals forces) which may further stabilize through chemisorption to form a donor type bond. Electron transfer from the adsorbed species is favoured by the presence of relatively loosely bound electrons such as in anions and neutral organic molecules containing lone pair electrons or  $\pi$ -electron systems associated with multiple bonds, especially triple, bonds or aromatic rings. In general, the organic inhibitors used have functional groups

which are sites for the chemisorption process. Lone pair electrons for coordinate bonding occur in functional groups containing elements of group V and VI of the Periodic table. The tendency to stronger co-ordinate bond formation (and hence stronger adsorption) by these elements increases with decreasing electronegativity in the order  $O < N < S < Se$  and depends on the nature of the functional groups containing these elements (Mansfield, 1987a).

The above sequence has also been explained on the basis of electron density and polarizability of the elements. On this basis, a surface bond of the Lewis acid-base type, normally with the inhibitor as electron donor and the metal as electron acceptor has been postulated. The hard and soft acid base theory has been applied to the corrosion inhibition phenomena with inhibitors being arbitrarily termed as 'hard' and 'soft' inhibitors. Softness and hardness are associated with high and low polarizability respectively. According to the hard and soft acid base (HSAB) principle, hard acids react with hard bases more readily than with soft bases. Neutral metal atoms are soft acids which tend to react with soft bases such sulphur-bearing inhibitors. Nitrogen-containing or oxygen-containing inhibitors are considered to be hard bases and may establish weaker bonds with metal surfaces (Mansfield, 1987a; Sastri, 1998c).

### 1.3.3 Mechanism of adsorption of inhibitors

The corrosion of metals in aqueous acidic solutions can be inhibited by a very wide range of substances including  $\text{CrO}_4^{2-}$ ,  $\text{MoO}_4^{2-}$  (Abd Rehim *et al.*, 2004; Wang *et al.*, 2004; Refaey, 2005), phosphates (Refaey, 2005), bismuth(III) compounds (Hayashi *et al.*, 1996) and organic compounds that contain nitrogen, sulphur, oxygen and multiple bonds in the molecules. These organic compounds have therefore continued to provoke research interests (Lagrene *et al.*, 2002; Branzoi *et al.*, 2002; Hosseini *et al.*, 2003; Lgamri *et al.*, 2003; Osman *et al.*, 2003; Maayta and Al-Rawashdeh, 2004; Ozcan *et al.*, 2004; Ravichandran *et al.*, 2004; Hui-Long *et al.*, 2004; Morales-Gil *et al.*, 2004; Ferreira *et al.*, 2004). It is often not possible to assign a single general mechanism of action to an inhibitor, because the mechanism may change with experimental conditions. Thus, the predominant mechanism of action of an inhibitor in acidic solutions may vary with factors such as concentration, the pH of the acid, the nature of the anion of the acid, the presence of other species in the solution, the extent of reaction to form secondary inhibitors and the nature of the metal (Shreir, 1978b).

The anodic and cathodic reactions involved in the corrosion of metal in acidic solutions are:



The adsorbed inhibitor blocks either the anodic or cathodic reaction or both. Adsorption is the primary step in achieving inhibition in acid solutions. This is a consequence of the fact that the corroding metal surface to be inhibited is usually oxide-free allowing the inhibitor ready access to retard the cathodic and/or the anodic electrochemical processes of corrosion. Once the inhibitor has adsorbed on the metal surface it can then affect the corrosion reactions in a number of ways: by offering a physical barrier to the diffusion of ions or molecules to or from the metal surface; direct blocking of anodic and/or cathodic reaction sites; interaction with corrosion reaction intermediates; change the make-up of the electrical double layer which develops at the metal/solution interface and so affect the rate of electrochemical reactions (Harrop, 1991).

The adsorbed inhibitor may not cover the entire metal surface, but occupies sites which are electrochemically active and thereby reduces the extent of anodic or cathodic reaction or both. The corrosion rate will be decreased in proportion to the extent to which the electrochemically active sites are blocked by the adsorbed inhibitor. Comparison of the electrochemical polarisation curves obtained both in the presence and absence of an inhibitor shows a shift of the polarisation curves in an inhibitor containing solutions to lower current density values without any change in Tafel slopes. This shows that there is no change in the reaction mechanism. Anodic dissolution of metals is assumed to be a stepwise reaction with adsorbed intermediates on the surface of the metal. In the anodic dissolution of iron, adsorbed intermediate FeOH is assumed and on addition of an organic inhibitor, a complex of the type [FeOH.I] adsorbed on the surface of iron is assumed. This surface complex changes the reaction

mechanism with an increase in the anodic Tafel slope (Shreir, 1978b; Mansfield, 1987a).

Inhibition of the corrosion of metals and alloys in near-neutral aqueous solutions has been achieved in many cases by using inorganic compounds (Refaey and Abd El Rehim, 1996; El Sherbini *et al.*, 2000; Abdel Rehim *et al.*, 2004; Amin, 2005) as well as organic compounds (Rocca *et al.*, 2001; Rocca and Steinmetz, 2001; Rocca *et al.*, 2004; Peultier *et al.*, 2003). The corrosion processes result in the formation of sparingly soluble surface products such as oxides, hydroxides, or salts. The cathodic partial reaction is oxygen reduction. In these cases, the inhibitor action will be exerted on the oxide-covered surface by increasing or maintaining the protective characteristics of the oxide or of the surface layers in the aggressive solutions. The displacement of preadsorbed water molecules by adsorbing inhibitor molecules may be usually considered the fundamental step of inhibition. Chemical or electrochemical reactions of the inhibitor at the surface may also be assumed in order to explain the inhibitor efficiency. Because of these reactions, additional inhibitor uptake may take place.

As a result of the adsorption of the inhibitor at the oxide-covered metal surface, there may be different inhibition mechanisms. Thick surface layers having poor electronic-conductive properties are found in the presence of inhibitors that restrict diffusion of oxygen; these additives interfere with the oxygen reduction reaction and are referred to as cathodic inhibitors. Additives giving rise to thin passivating films usually inhibit the anodic metal dissolution reaction; as a

consequence, these types of inhibitors are considered anodic inhibitors (Mansfield, 1987a).

Mansfield (1987a) further remarked that the mechanism of action of both inorganic and organic inhibitive anions on the corrosion of various metals such as Fe, Al, and Zn in near-neutral solutions involves the following:

- Stabilization of the passivating oxide film by reducing its dissolution rate
- Repassivation of the surface due to repair of the oxide film by promoting re-formation of the oxide
- Repair of the oxide film by formation of insoluble surface compounds and consequent plugging of pores
- Prevention of the adsorption of aggressive anions because of the competitive adsorption of inhibitive anions.



#### 1.4 Methods of evaluations of corrosion inhibition

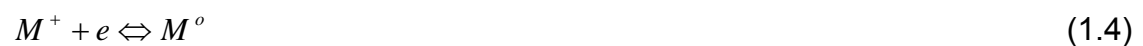
Good reproducibility of the levels of inhibition in test procedures is rendered difficult due to the complexity of the factors controlling corrosion and its inhibition. These factors include the surface condition of the metal, temperature and the composition of the environment. Similar difficulties exist in the assessment of corrosion and its inhibition. Since corrosion inhibitors are used in a wide range of applications, no universal test method is possible. Even within one type of application there will be a range of requirements and a diversity of opinions on the definition of effective inhibition.

Measurement of mass loss is probably the widely used method of inhibition assessment. However care is required in both the technique and the interpretation of results. In the solution analysis method, determinations are made of the changes with time in the content of metal ions measured and inhibition will be reflected in the analytical data. There are also published tests methods, often referred to as standard test methods. These test methods are identified by numbered documents such as the salt spray (fog) corrosion test which is given in ASTM B117. The electrochemical methods which are applied to liquid phase systems include the measurement of electrode potential, polarisation of electrode reactions, galvanic currents, electrical resistance, capacitance, ac impedance techniques and noise measurements (Mercer, 1985). However, mass loss measurements (Lagreneee *et al.*, 2002; El Azhar *et al.*, 2002; Abd. El-Maksoud, 2002 ; Hui-Long *et al.*, 2004; Maayta *et al.*, 2004; Ravichandran *et al.*, 2004; Ferreira *et al.*, 2004) polarisation measurements

(Tommesani *et al.*, 1997 ; Vracar and Drazic, 2002 ; El Azhar *et al.*, 2002; Abd. El-Maksoud, 2002; Hosseini *et al.*, 2003; Popova *et al.*, 2003; Quraishi and Jamal, 2003 ; Osman *et al.*, 2003 ; Hui-Long *et al.*, 2004; Maayta *et al.*, 2004; Ozcan *et al.*, 2004; Ravichandran *et al.*, 2004;) and ac impedance techniques (Tommesani *et al.*, 1997; El Azhar *et al.*, 2002; Abd. El-Maksoud, 2002; Yadaf *et al.*, 2004; Lgamri *et al.*, 2003; Hosseini *et al.*, 2003; Popova *et al.*, 2003; Ravichandran *et al.*, 2004; Ozcan *et al.*, 2004) remained as the commonly used methods of evaluation.

#### 1.4.1 Stern-Geary theory

Most modern corrosion techniques are based on the theoretical analyses of the shape of polarisation curves by Stern and Geary which was first introduced in 1957 (Stern and Geary, 1957) and since then has been expended and developed (Sastri, 1998a). In a simple non-corroding system containing M and  $M^+$  at equilibrium:



$$i_{R,M} = i_{O,M} = i_{ex} \quad (1.5)$$

where  $i_{R,M}$  is the current for reduction of  $M^+$

$i_{O,M}$  is the current for oxidation of M

$i_{ex}$  is the exchange current (similar to  $i_{corr}$  in a corrosion process)

If a potential is applied on the metal from an external source and the reaction rate is controlled by a slow chemical step that requires an activation energy:

$$i_{R,M} = i_{ex} e^{-\eta/\beta} \quad (1.6)$$